HHS Public Access

Author manuscript

Nanotoxicology. Author manuscript; available in PMC 2017 July 02.

Published in final edited form as:

Nanotoxicology. 2017 March ; 11(2): 278–288. doi:10.1080/17435390.2017.1293750.

Reactive Oxygen Species Generation by Copper(II) Oxide Nanoparticles Determined by DNA Damage Assays and EPR Spectroscopy

Carlos Angelé-Martínez[1], **Khanh Van T. Nguyen**[2], **Fathima S. Ameer**[1], **Jeffrey N. Anker**[1], and **Julia L. Brumaghim**[*,1]

[1]Department of Chemistry, Clemson University, Clemson, SC 29634-0973, USA

[2]School of Biotechnology, International University - Vietnam National University Ho Chi Minh City, Ho Chi Minh, Vietnam

Abstract

Copper(II) oxide nanoparticles (^{NP}CuO) have many industrial applications, but are highly cytotoxic because they generate reactive oxygen species (ROS). It is unknown whether the damaging ROS are generated primarily from copper leached from the nanoparticles, or whether the nanoparticle surface plays a significant role. To address this question, we separated nanoparticles from the supernatant containing dissolved copper, and measured their ability to damage plasmid DNA with addition of hydrogen peroxide, ascorbate, or both. While DNA damage from the supernatant (measured using an electrophoresis assay) can be explained solely by dissolved copper ions, damage by the nanoparticles in the presence of ascorbate is an order of magnitude higher than can be explained by dissolved copper and must therefore depend primarily upon the nanoparticle surface. DNA damage is time-dependent, with shorter incubation times resulting in higher EC_{50} values. Hydroxyl radical is the main ROS generated by ^{NP}CuO/hydrogen peroxide as determined by EPR measurements; ^{NP}CuO/hydrogen peroxide/ascorbate conditions generate ascorbyl, hydroxyl, and superoxide radicals. Thus, ^{NP}CuO generate ROS through several mechanisms, likely including Fenton-like and Haber-Weiss reactions from the surface or dissolved copper ions. The same radical species were observed when ^{NP}CuO suspensions were replaced with the supernatant containing leached copper, washed ^{NP}CuO, or dissolved copper solutions. Overall, ^{NP}CuO generate significantly more ROS and DNA damage in the presence of ascorbate than can be explained simply from dissolved copper, and the ^{NP}CuO surface must play a large role.

Keywords

Nanoparticles; nano-surfaces; nanotoxicology; DNA damage

[*]Corresponding author: Tel: + 1 864 656 0481; fax + 1 864 656 6613, brumagh@clemson.edu.

Declaration of interest: The authors report no conflicts of interest. The authors alone are responsible for the content and writing of the paper.

Author Manuscript Author Manuscript Author Manuscript Author Manuscript

Author Manuscript Author Manuscript Author Manuscript Author Manuscript

Introduction

Copper(II) oxide nanoparticles (^{NP}CuO) are used as antimicrobial agents in textiles (Ren *et al.* 2009) and paints (Cooney 1995), as catalysts in organic synthesis (Alves *et al.* 2009), in the oxidation of pollutants (Moshe *et al.* 2009), and they are also generated from electronics waste. Unfortunately, industrial use of ^{NP}CuO represents a potential health and environmental concern because the particles are toxic and mutagenic. While copper ion toxicity is attributed to reactive oxygen species (ROS) generation, (Angelé-Martínez 2014; Gaetke 2014) nanoparticle toxicity mechanisms could differ due to surface chemistry and differences in uptake and distribution at the organismal and cellular levels.

Hydrogen peroxide (H_2O_2), superoxide ($O_2^{\bullet -}$), hydroxyl radical ($^{\bullet}OH$), and singlet oxygen ($^1O_2$) are common ROS, and their interactions with DNA, proteins, and lipids cause oxidative damage and cell death (Bondarenko *et al.* 2013; Maurer-Jones *et al.* 2013). Oxidative DNA damage is the primary cause of cell death and mutation in aging, cancer, neurodegeneration, and cardiovascular disease (Burgess *et al.* 2012; Cooke *et al.* 2003; Ide *et al.* 2001; Keyer *et al.* 1995; Luijsterburg and Van Attikum 2011). Nanoparticles are internalized into bacteria and human cells where they localize in mitochondria and the nucleus (Cronholm *et al.* 2013; Wang *et al.* 2012) and potentially damage DNA. Reviews on nanoparticle toxicity call for immediate research to 1) understand the uptake, metabolism, accumulation, and secretion of nanoparticles; 2) develop predictive toxicity models and classify nanoparticles according to their toxicity; and 3) prevent health issues caused by nanoparticle exposure (Bondarenko *et al.* 2013; Rim *et al.* 2013).

^{NP}CuO are among the most toxic nanoparticles (Bondarenko *et al.* 2013). In a comparative toxicity assay, ^{NP}CuO caused significant mitochondrial depolarization (Karlsson *et al.* 2009) and increased DNA damage compared to carbon nanotubes and nanoparticulate TiO_2, ZnO, CuZn, Fe_3O_4, and Fe_3O_4 (Karlsson, Cronholm, *et al.* 2008). Many factors influence ^{NP}CuO toxicity, including pH, exposure time, dose, zeta potential, solubility, size, porosity, morphology and surface area (Cho *et al.* 2012; Grassian 2008; Karlsson *et al.* 2009; Luyts *et al.* 2013). Although a few reports indicate minimal toxicity upon ^{NP}CuO exposure under certain conditions (Karlsson, Cronholm, *et al.* 2008; Karlsson *et al.* 2009; Wang *et al.* 2012), ^{NP}CuO are more toxic to cells than bulk CuO (Wang *et al.* 2012) or polymeric CuO (Thit *et al.* 2013).

^{NP}CuO can generate DNA-damaging ROS by two primary mechanisms: at the nanoparticle surface or in solution by copper dissolved from the nanoparticle surface. In both cases, the site of ROS generation must be in close proximity to damage DNA due to the short lifetimes of these ROS. Although these two mechanisms are known (Karlsson, Cronholm, *et al.* 2008; Studer *et al.* 2010), the amount of damage contributed by each component and the details that control these mechanisms are not well understood.

Dissolved copper ions are reportedly more toxic to aquatic organisms than the same number of copper atoms in a copper oxide nanoparticle (Blinova *et al.* 2010; Bondarenko *et al.* 2013; Jo *et al.* 2012) since many copper atoms reside within the particle core. Nonetheless, ^{NP}CuO are highly toxic, in part because the large surface-area-to-volume ratio allows rapid copper

Author Manuscript Author Manuscript Author Manuscript Author Manuscript

dissolution from ^{NP}CuO, especially compared to bulk CuO (Bondarenko *et al.* 2013; Kasemets *et al.* 2009; Shi *et al.* 2011), and because the ^{NP}CuO surface can also generate ROS (Cho *et al.* 2012). In a Trojan horse effect (Wang *et al.* 2012), ^{NP}CuO uptake results in orders-of-magnitude greater copper uptake and accumulation in mammalian cells and correspondingly greater DNA damage and cell death than for dissolved copper (Cronholm *et al.* 2013). ^{NP}CuO uptake depends strongly upon nanoparticle size and surface chemistry, including binding and adsorption to biomolecules (Maurer-Jones *et al.* 2013). Generally, smaller nanoparticles are more toxic, due to a combination of increased surface area, increased copper dissolution rates, and/or increased nanoparticle uptake (Karlsson *et al.* 2009). Increased toxicity with decreased size is observed in crustaceans (Blinova *et al.* 2010) and duckweed treated with ^{NP}CuO and bulk CuO (Shi *et al.* 2011).

Most research on ^{NP}CuO toxicity has been performed in bacteria and mammalian cells or whole organisms to examine cell growth inhibition, DNA damage, and apoptosis. No in vitro studies have directly assessed the chemical mechanisms of ^{NP}CuO-induced toxicity. Our in vitro analysis of ^{NP}CuO-mediated DNA damage focuses specifically on oxidative DNA damage as an endpoint, directly relating to mechanisms responsible for mutagenesis, oncogenesis, and cell-death processes, without confounding effects from cellular oxidative stress responses, nanoparticle internalization processes, and adsorption of cellular molecules. This work presents the analysis of DNA damage caused by ^{NP}CuO and its undissolved (^{w}CuO) and dissolved (^{l}CuO) fractions in the presence of H_2O_2 and/or ascorbate to determine the damaging effects of ^{NP}CuO, dissolved copper, and ^{NP}CuO surface reactions. Electron paramagnetic resonance (EPR) spectroscopy was used to detect ROS generation by ^{NP}CuO or dissolved copper in the presence of H_2O_2 and/or ascorbate. Our results indicate that ^{NP}CuO and dissolved copper generate ROS by different mechanisms and that the ^{NP}CuO surface plays a significant role in ROS generation.

Materials and Methods

Materials

Water was purified using a Barnstead NANOpure DIamond Life Science water deionization system. 3-Morpholinopropane-1-sulfonic acid (MOPS; Alfa Aesar), $CuSO_4$ (Fisher), L-(+)-ascorbic acid (99+%; Alfa Aesar), Chelex 100 resin (Sigma-Aldrich), and disodium dihydrogen ethylenediaminetetraacetate (EDTA; TCI America) were used as received. CuO nanoparticles (50% weight, U1121W Nanophase Technologies Corporation, distributed through Alfa Aesar/Sigma-Aldrich) were used as received to prepare diluted suspensions. These particles were selected because they are formed by plasma oxidation of copper, which provides a high-purity product, and the same particles were used in several toxicity assays (Kartal *et al.* 2009; Selvakumar and Suresh 2012) and in studies of heat transfer fluids (Selvakumar and Suresh 2012; Vajjha *et al.* 2010). The ^{NP}CuO suspensions also contained a proprietary dispersant added by the manufacturer. Microcentrifuge tubes were rinsed in 1 M HCl, triply rinsed in deionized H_2O, and dried prior to use. Buffered solutions were treated with Chelex resin (2 g/80 mL buffer) for 24 h prior to use. $CuSO_4$ and ascorbate solutions were prepared prior to each experiment and used immediately.

Author Manuscript Author Manuscript Author Manuscript Author Manuscript

Characterization of CuO nanoparticles

Transmission electron microscope (TEM) images of ^{NP}CuO were acquired using a Hitachi TEM H7600 microscope under 115 kV and 300,000× direct magnification. The ^{NP}CuO crystal domain size was calculated from its X-ray diffraction spectrum measured by a Rigaku Ultima IV X-ray diffractometer with $K_{\alpha 1}$(Cu) radiation with a tube voltage and current set at 40 kV and 40 mA, respectively. The average hydrodynamic diameter and zeta potential of ^{NP}CuO in MOPS (pH 7) buffer and deionized water were determined using dynamic light scattering with a Malvern Zetasizer Nano ZS instrument.

Determination of dissolved copper using the bathocuproine method

^{NP}CuO (50% wt. in water) was diluted in MOPS buffer (35 mM, pH 7) to make 5 mM ^{NP}CuO. The suspension was sonicated for 5 min, centrifuged (13000 rpm/~18000 g RCF for 10 min), and the leachate was separated. The leachate was centrifuged at least three times to ensure ^{NP}CuO were removed, and then diluted 10× before mixing with Cu(II) standards (1:1 ratio) and bathocuproine reagents (Eaton *et al.* 2001) with a scale-down ratio of 3/50. The resulting orange copper-bathocuproine complex absorbance was measured in triplicate using an Agilent 8453UV-vis spectrophotometer. The concentration of dissolved copper in the ^{NP}CuO leachate was determined using standard addition with Cu(II) standard solutions of 0.5, 0.25, 0.125, and 0.0625 mg/L (Tables S1, S2 and Figure S1). The bathocuproine method was validated using flame atomic absorption spectroscopy, which gave results for several samples within 10%.

Transfection, amplification, and purification of plasmid DNA

Plasmid DNA (pBSSK) was purified from *E. coli* strain DH1 using a PerfectPrep Spin kit (Fisher), then dialyzed at 4 °C against EDTA (1 mM) and NaCl (50 mM) for 24 h and then against NaCl (130 mM) for 24 h to remove metal ions. Absorbance ratios for DNA solutions were A_{250}/A_{260} 0.95 and A_{260}/A_{280} 1.8.

Plasmid DNA damage assays with ^{NP}CuO, ascorbate and H_2O_2

A solution containing NaCl (130 mM), MOPS (pH 7, 10 mM), and ethanol (10 mM) as a radical scavenger (Henle *et al.* 1999) was combined with ^{NP}CuO, ^{l}CuO, or ^{w}CuO (1.0 – 1000 μM) and ascorbate (0.00125 – 1250 μM) as indicated in Table 1. MOPS buffer was used since it does not chelate copper, and 1.25 molar equivalents of ascorbate were used to ensure that all Cu^{2+} was reduced to $^{\bullet}OH$-generating Cu^{+}. Buffer pH was essentially unaffected even at the highest ascorbate concentrations. After 5 min, plasmid DNA (pBSSK, 0.1 pmol in 130 mM NaCl) was added, and the solution was allowed to stand for 5 min before H_2O_2 (50 μM) addition to give a 10 μL total volume. After 30 or 150 min, EDTA (200 mM, 0.5 μL) and loading dye (2 μL) were added. Dissolved copper gels were performed with $CuSO_4$ solutions instead of ^{NP}CuO suspensions.

Gel electrophoresis was run on a 1% agarose gel in TAE buffer for 60 min at 140 V to separate nicked (damaged) and supercoiled (undamaged) plasmid DNA. Gels were stained with ethidium bromide for 5 min and washed in water for an additional 10 min before imaging under UV light. Intensities of the damaged and undamaged DNA bands were quantified using UVIproMW software (Jencons Scientific, Inc.). Ethidium bromide stains

supercoiled DNA less efficiently than nicked DNA, so supercoiled DNA band intensities were multiplied by 1.24 prior to comparison (Hertzberg and Dervan 1982). Intensities of the nicked and supercoiled bands were normalized for each lane so that % nicked + % supercoiled = 100 %.

CuO nanoparticle treatment for plasmid DNA damage assays

Separation of undissolved and dissolved fractions of ^{NP}CuO is described in Figure 1. Briefly, freshly prepared ^{NP}CuO stock solution (5.0 mM in MOPS buffer) was sonicated for 10 min. An aliquot (4 mL) of the ^{NP}CuO suspension was centrifuged (13000 rpm, ~18000 g, 10 min) to separate the leachate (^{l}CuO) from the solid. The leachate was removed, and the solid was resuspended in deionized water (at the same volume as the ^{l}CuO) and centrifuged again. The supernatant was discarded, and the ^{w}CuO were resuspended in deionized water and re-sonicated (5 min). All fractions (^{NP}CuO, ^{l}CuO, and ^{w}CuO) were diluted based upon the original concentration of ^{NP}CuO (5.0 mM) and shaken for three seconds to ensure homogeneity before use in DNA damage assays.

Removal of dissolved copper from the leachate of CuO nanoparticles (^{l}CuO)

CuO nanoparticles were separated from the suspensions by centrifugation at 14,000 rpm (30,074 RCF) for 45 min. The supernatant was removed and re-centrifuged ~10 times to ensure complete removal of ^{NP}CuO. A saturated $(NH_4)_2CO_3$ solution (200 μL) was mixed with ^{NP}CuO supernatant (1 mL), and the resulting mixture was agitated for ~1 min using a vortex mixer. The deep-blue-colored solution was then heated until most of the dissolved copper precipitated, and the supernatant was separated by filtration (Europe 25 mm syringe filter with a 0.2 μm PTFE membrane). Any remaining dissolved copper was removed by treating the supernatant with Chelex resin for 24 h.

Statistical Analysis

Percent DNA damage was plotted with respect to ^{NP}CuO, ^{l}CuO, ^{w}CuO, or Cu^{2+} concentrations on a semi-log plot and fit to a sigmoidal dose-response curve with maximum damage set to 100%. Data are reported as average values with standard deviations from three independent experiments. EC_{50} values were calculated by fitting all points of three trials with a single curve (the mean of the EC_{50} fits from each trial gives similar results to the pooled data, 0–3% difference, but the pooled data should be less sensitive to noise). EC_{50} value standard deviations were calculated from the three trials' individual EC_{50} values. Data in Table S17, line 7 represent the average of two values, since the third gel showed an outlier value and was discarded. The relative standard deviation for the EC_{50} results was around 11% (average for 20 experiments with reported EC_{50}) and the largest relative standard deviation was 28%. Since the triplicate studies used for calculating standard deviation were performed at close to the same time, uncertainty may be larger in comparing different reaction conditions acquired at different times. Finally, for some curve shapes, the three-parameter fit can be especially sensitive to single points and there are cases where the standard deviation of three trials may underestimate the noise. Based upon these considerations, we consider that the standard deviations somewhat overestimate the accuracy, and we generally do not consider average EC_{50} differences of < 33% to be significant and chemically important.

Author Manuscript Author Manuscript Author Manuscript Author Manuscript

Author Manuscript Author Manuscript Author Manuscript Author Manuscript

Electron paramagnetic resonance (EPR) spectroscopy

EPR spectra were acquired on a Bruker EMX spectrometer using a quartz flat cell at room temperature using a 2,2-diphenyl-1-picrylhydrazyl (DPPH; g = 2.0036 (Mani *et al.* 2004)) standard centered at 3500 G with a sweep width of 100 G. The modulation amplitude was between 0.50 and 1.00 G, time and conversion constants were 81.92 s; and microwave power and frequency were 20.02 mW and 9.752 GHz, respectively. Samples (500 μL) were prepared in a MOPS buffer solution (10 mM, pH 7) containing ^{NP}CuO, ^{w}CuO, or ^{l}CuO (300 μM) with ascorbate (375 μM), 5,5-dimethyl-1-pyrroline-*N*-oxide (DMPO, 30 mM) as a spin trap, and H_2O_2 (22.5 mM, added last) and measured in less than 5 min.

Results

CuO nanoparticles were first characterized by dynamic light scattering/zeta potential, electron microscopy, and X-ray diffraction. We also measured the dissolved copper concentration in the suspensions. The whole ^{NP}CuO suspension, the supernatant alone, or washed and resuspended ^{NP}CuO were then incubated with DNA, and electrophoresis was performed to determine the percentage of damaged DNA for different nanoparticle concentrations with or without addition of hydrogen peroxide and/or ascorbate (Figure 1). Finally, EPR spectroscopy was performed to determine the ROS generated by ^{NP}CuO under various conditions and correlated to the observed DNA damage.

CuO Nanoparticle Characterization

^{NP}CuO were characterized with transmission electron microscopy (TEM), X-ray diffraction (XRD), dynamic light scattering (DLS), and zeta potential analyses. The amount of copper dissolved from ^{NP}CuO was measured by UV-vis absorption using the bathocuproine method (Eaton *et al.* 2001). TEM images show that ^{NP}CuO are roughly spherical, with a diameter of 50 – 60 nm (Figure S1). The crystal domain size of ^{NP}CuO, calculated from its XRD spectrum (Figure S2) using the Scherrer equation (Scherrer 1918), is 20 – 30 nm. XRD results also confirm that the ^{NP}CuO contained no crystalline impurities. The average hydrodynamic diameter of ^{NP}CuO in MOPS buffer (pH 7) measured by DLS is ~200 nm weighted by intensity, 146 nm weighted by volume, and ~98 nm weighted by particle number (Table S1 and Figure S3). ^{NP}CuO appear to be moderately well-dispersed in water with a zeta potential of −28 mV (Figure S4). A proprietary dispersant, likely similar to a polyethylene glycol as determined by infrared spectroscopy (data not shown), was added to the ^{NP}CuO suspensions by the manufacturer.

Concentrations of dissolved copper in the nanoparticle leachate (^{l}CuO) were determined using the standard addition method. A representative calculation for copper release from ^{NP}CuO in MOPS buffer is shown in Table S2 and Figure S4. Time dependence of dissolved copper concentrations from ^{w}CuO in buffer and from ^{NP}CuO suspension in buffer with ascorbate are presented in Figure S4C. The dissolved copper concentration is linear up to 150 min, and dissolved copper from ^{w}CuO is about half that of ^{NP}CuO. The concentration of dissolved copper measured using the bathocuproine method (0.5% the concentration of ^{NP}CuO) is consistent with previous reports (Atha *et al.* 2012; Gunawan *et al.* 2011). Dissolved copper concentrations increase with time (Kasemets *et al.* 2009; Studer *et al.*

Author Manuscript Author Manuscript Author Manuscript Author Manuscript

2010) and with lower pH (Bondarenko *et al.* 2013; Cho *et al.* 2012; Grassian 2008; Studer *et al.* 2010); ascorbate may increase dissolved copper concentrations by lowering pH and chelating copper from the ^{NP}CuO surface.

DNA damage by CuO nanoparticles under oxidative stress conditions

We performed an in vitro plasmid DNA damage assay to measure CuO-mediated damage since DNA damage is intimately related to cell mutagenesis and death (Keyer *et al.* 1995; Luijsterburg and Van Attikum 2011). Plasmid DNA damage conditions were selected to produce single-strand nicks in the DNA backbone, resulting in closed, circular plasmids in distinct bands that are easily separated from undamaged, supercoiled DNA by gel electrophoresis. This technique is simpler than lipid and protein oxidation experiments, which require longer treatment times, more rigorous separation techniques, and identification of multiple oxidation products.

To compare DNA damage from ^{NP}CuO suspension, washed ^{NP}CuO suspension (^{w}CuO), or leachate solution (^{l}CuO; Figure 1), each of these components was combined with plasmid DNA, H_2O_2 and/or ascorbate for either 30 or 150 min. Electrophoresis was then performed to separate damaged from undamaged DNA. Figure 2A shows the gel electrophoresis image of plasmid DNA treated with H_2O_2 and increasing concentrations of ^{NP}CuO. DNA is undamaged upon treatment with H_2O_2 or ^{NP}CuO alone (lanes 2–3), and DNA treated with $CuSO_4$ (6 μM, lane 4), ascorbate (7.5 μM), and H_2O_2 (50 μM) produces damaged DNA in the positive control. As ^{NP}CuO concentration increases with a fixed H_2O_2 concentration (50 μM; lanes 5 to 13), DNA damage increases until essentially all plasmids are damaged. The percentage DNA damage was quantified by integrating the gel band intensities. By fitting ^{NP}CuO concentration vs. DNA damage percentage with a sigmoidal dose-response curve (Figure 2B), the EC_{50} value for ^{NP}CuO-mediated DNA damage was calculated as 324 μM (Table 1). At least 21 different DNA damage conditions were tested, each in triplicate, and EC_{50} values are shown in Table 1. DNA damage data tables and representative gels for each experiment are shown in the supporting information (Tables S5–25 and Figures S5–25).

Table 1 shows both the EC_{50} values for and the estimated dissolved copper in each sample. Separate concentrations are given for unwashed ^{NP}CuO suspensions (that have stabilized after long-term incubation in solution) and for the supernatant (^{l}CuO, where no nanoparticles are present to leach copper). In conditions where we observed continuous copper leaching into the solution (i.e., immediately after nanoparticle washing, or after addition of ascorbate), we give a range corresponding to the smallest initial and largest final concentration we measured during incubation (Figure S4). Copper dissolution rates were approximately the same at 30 and 60 μM ascorbate (where the EC_{50} was observed), but there is concentration dependence, e.g., copper dissolution rates are slower at very high or low concentrations.

For several reaction conditions, DNA damage was measured at both 30 and 150 minutes (Figure 3). Figure 4 shows the EC_{50} curves for ^{NP}CuO trials at 30 and 150 minutes. The EC_{50} value for DNA damage decreased with incubation time for all cases with the same initial conditions at 30 and 150 min. However, damage was not generally proportional to time, indicating higher order reaction rates (also supported by the Hillslope being >1 for all

Author Manuscript Author Manuscript Author Manuscript Author Manuscript

21 reaction conditions). Experiments with $^{w}CuO + H_2O_2$, $^{l}CuO + H_2O_2$, or $^{l}CuO + H_2O_2$ + ascorbate were not performed as they were unnecessary to establish the effects of both nanoparticle components, and the resulting EC_{50} values for these conditions are expected to be well above expected physiological and environmental copper concentrations (Stockel *et al.* 1998) based on the trends observed for EC_{50} values determined for ^{NP}CuO + H_2O_2, ^{NP}CuO + ascorbate/H_2O_2, and ^{w}CuO + ascorbate + H_2O_2 conditions.

EPR detection of radicals

Electron paramagnetic resonance (EPR) spectroscopy was used to detect and identify ROS generated by ^{NP}CuO, ^{w}CuO, and ^{l}CuO under conditions similar to those used in the DNA damage assays (i.e. with H_2O_2, ascorbate, and both components together). Due to the short lifetime of ROS, 5,5-dimethyl-1-pyrroline-*N*-oxide (DMPO) was added as a spin trap, since DMPO adducts of superoxide ($O_2^{\bullet -}$) and hydroxyl radical ($^{\bullet}OH$) are readily distinguishable (Bartosz 2006; Villamena and Zweier 2004). Ascorbyl radical can be directly observed, and to detect singlet oxygen ($^{1}O_2$), the 2,2,6,6-tetramethyl-piperidine (TEMP) spin trap was used (Fufezan *et al.* 2002).

The EPR spectrum of ^{w}CuO with H_2O_2 (Figure 5A) exhibits the characteristic quartet resonance of the DMPO-OH adduct (Villamena and Zweier 2004), indicating $^{\bullet}OH$ formation. Combining ^{w}CuO and ascorbate (Figure 5B) results in an EPR spectrum with only the ascorbyl radical resonance observed (A = 1.9 G) (Mouithys-Mickalad *et al.* 1998). Adding both ascorbate and H_2O_2 to ^{w}CuO, yields an EPR spectrum with resonances for the DMPO-OH adduct, ascorbyl radical, and a DMPO-OOH adduct derived from reaction with superoxide (Figure 5C). The DMPO-O_2 adduct decomposes rapidly to DMPO-OOH, which in turn decomposes to generate DMPO-OH (Clément *et al.* 2004).

Comparing results from the three CuO fractions (^{NP}CuO, ^{w}CuO, and ^{l}CuO), we find that the type of ROS detected depends upon whether H_2O_2, ascorbate, or both are added, but not upon which nanoparticle fraction is added (Figure 6). The EPR instrument displayed day-to-day drift in the magnetic field, causing minor shifts in peak positions, and signal intensities varied somewhat according to sample placement and instrument drift. However, changes in the shape of the spectra are significant and due to changes in relative amounts of each radical detected.

To investigate whether superoxide was generated, the EPR spectrum of K_2O (a superoxide salt) was acquired under the same conditions. The EPR spectrum shows only the DMPO-OH resonance (data not shown), indicating rapid superoxide decomposition to $^{\bullet}OH$. In addition, the EPR spectrum of $Cu^{2+} + H_2O_2$ with DMPO also shows a very low-intensity DMPO-OOH adduct resonance (Figure 7A), confirming superoxide generation under these conditions. Although singlet oxygen formation was confirmed in $Cu^{2+} + H_2O_2$ + ascorbate samples using the TEMP spin trap (Figure 7B), similar experiments conducted on Cu^{2+} + ascorbate, $Cu^{2+} + H_2O_2$, or nanoparticle-containing samples with TEMP showed no evidence of $^{1}O_2$ generation. These results indicate that although $^{1}O_2$ is detected in positive controls using our EPR conditions, the ^{NP}CuO samples do not generate $^{1}O_2$ in detectable concentrations.

Author Manuscript Author Manuscript Author Manuscript Author Manuscript

Discussion

Experiments were designed to determine to what extent the nanoparticle surface plays a role in nanoparticle-mediated damage. Figure 3 shows the general approach, where the nanoparticles, washed particles, and supernatant were separately tested for DNA damaging ability. It also shows one of the most striking results: in the presence of ascorbate and hydrogen peroxide, the EC_{50} was an order of magnitude higher for the ^{NP}CuO than could be explained by dissolved copper. At the EC_{50} concentration, dissolved copper in the ^{NP}CuO suspensions ranged from 0.09 μM at the start of the reaction to ~0.27 μM by the end; this range in dissolved copper is due to the gradual dissolution of copper oxide in the presence of ascorbate (Figure S4). In comparison, for dissolved copper from $CuSO_4$, the EC_{50} value was 1.6 μM, implying the ^{NP}CuO is approximately an order or magnitude more damaging than would be expected from the dissolved copper in the sample. To confirm this effect, we repeated similar experiments under multiple conditions (Table 1).

Dissolved copper from $CuSO_4$ and ^{I}CuO

Copper is well known to generate ROS and damage DNA through Fenton-like and other reactions (Angelé-Martínez 2014). We observe that Cu^{2+} damages DNA in presence of H_2O_2, ascorbate, or both (Table 1). In the presence of both ascorbate and hydrogen peroxide, copper is reduced to Cu^+ that then reacts with H_2O_2 to generate hydroxyl radical in the Fenton-like reaction (Reaction 1). With only a reductant present (ascorbate), Cu^{2+} is less damaging than in the presence of H_2O_2 or both H_2O_2 + ascorbate (Table 1).

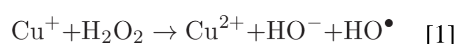

$$Cu^{+}+H_2O_2 \rightarrow Cu^{2+}+HO^{-}+HO^{\bullet} \quad [1]$$

To compare the effects of the nanoparticles and the dissolved copper in the nanoparticle suspensions, the nanoparticles were removed, leaving a supernatant containing dissolved copper and an organic dispersant (^{I}CuO). The EC_{50} for these ^{I}CuO samples, based upon dissolved copper measured in the supernatant, was expected to be close to the values for $CuSO_4$-derived dissolved copper, or slightly higher if the dispersant was a mild antioxidant. Indeed, the EC_{50} value for ^{I}CuO with ascorbate and H_2O_2 was 1.6 ± 0.2 μM at 150 minutes incubation (compared to 1.6 ± 0.2 μM for $CuSO_4$; Table 1) and 2.1 ± 0.2 μM at 30 minutes (compared to 2.3 ± 0.2 μM for $CuSO_4$). We also removed copper from the supernatant, and then spiked $CuSO_4$ back in (Table 1, Cu^{2+}/Other Conditions). Under these conditions, the EC_{50} value was 2.3 μM, similar to, but somewhat higher than, the value for $CuSO_4$ without the supernatant (1.6 μM). Taken together, these results establish that DNA damage from ^{I}CuO can be accounted for by the amount of dissolved copper in solution. Therefore, significant additional damage observed for ^{NP}CuO suspensions must be caused directly by the nanoparticles, not copper leached from the nanoparticles.

Colloidal suspension (^{NP}CuO) and washed nanoparticles (^{W}CuO)

From the data presented in Table 1, the DNA damage from ^{NP}CuO + H_2O_2 at 150 min (EC_{50} = 324 ± 29 μM) is similar to the damage expected from the dissolved copper measured in

Author Manuscript Author Manuscript Author Manuscript Author Manuscript

solution (1.54 μM dissolved copper in ^{NP}CuO, nearly identical to the EC_{50} value of 1.5 μM for Cu^{2+}). At only 30 min incubation, no significant DNA damage is observed under these conditions, and it was therefore not possible to test the contributions of ^{w}CuO and ^{l}CuO under similar conditions. In contrast, DNA damage by ^{NP}CuO in the presence of either ascorbate alone or ascorbate + H_2O_2 is an order of magnitude greater than can be explained by the dissolved copper in the ^{NP}CuO suspensions for both time points (Table 1).

To determine the ability of the nanoparticles alone to damage DNA, ^{NP}CuO were separated from the supernatant by centrifugation and washed to remove dissolved copper in the supernatant (Figure 1). These washed nanoparticles had less than half the dissolved copper compared to ^{NP}CuO suspensions, although dissolved copper from ^{w}CuO increased during incubation with ascorbate at a similar rate to ^{NP}CuO (Figure S4C). The ^{NP}CuO were consistently more damaging than ^{w}CuO, although this effect is smaller at 30 minutes (Table 1). Both ^{NP}CuO and ^{w}CuO generated significantly higher DNA damage compared to the amount of dissolved copper measured in solution in the presence of ascorbate or ascorbate + H_2O_2. In both cases, the EC_{50} value was far lower with ascorbate alone than with H_2O_2 alone. Adding both H_2O_2 and ascorbate gave EC_{50} values similar to but generally lower than ascorbate alone. There is one exception to this rule: for ^{w}CuO, the EC_{50} value at 30 minutes is 25% higher with H_2O_2 than without it; however, this is likely due to experimental error, since the EC_{50} curve with ascorbate and H_2O_2 (Figure S20 and Table S20) is especially noise-sensitive and the “true value” may be lower. Although H_2O_2 and ascorbate generally appear to be more damaging than either on their own, we cannot determine from these data to what extent the effect is synergistic or additive.

Possible Mechanisms

To elucidate mechanisms behind differences in DNA damaging ability, ROS produced by both the nanoparticles and dissolved copper was determined by EPR spectroscopy under conditions similar to electrophoresis experiments. All CuO fractions (^{l}CuO, ^{NP}CuO, and ^{w}CuO) produce radicals under DNA-damaging conditions, including $^{\bullet}$OH in the presence of H_2O_2, ascorbyl in the presence of ascorbate, both species when both ascorbate and H_2O_2 are added, and a DMPO-OOH adduct derived from superoxide formation.

H_2O_2—^{NP}CuO and ^{l}CuO have similar EC_{50} values in the presence of H_2O_2 (Table 1), and most of the DNA damage can be accounted for by reaction of H_2O_2 with dissolved copper to generate DNA-damaging $^{\bullet}$OH (Reaction 1) (Angelé-Martínez 2014). EPR spectra detect $^{\bullet}$OH consistent with this mechanism (Figures 5 and 6).

Ascorbate—The EC_{50} values for ^{NP}CuO and ^{w}CuO are about an order of magnitude lower than expected from the dissolved copper in the supernatant, and need to be explained by additional mechanisms relating to the nanoparticle surface. It is unlikely that DNA adsorbs on the ^{NP}CuO surface due to their negative zeta potential (−28 mV), so ROS generated on the nanoparticle surface would likely damage DNA close to the nanoparticle. EPR spectra show that ascorbyl radical (AscH$^{\bullet}$) was produced. Since AscH$^{\bullet}$ is a weak oxidant, it is unlikely that it directly damages DNA (Iyanagi *et al.* 1985; Valko *et al.* 2005). However,

Author Manuscript Author Manuscript Author Manuscript Author Manuscript

$AscH^•$ is a better reducing agent than ascorbate (Cadena 1997) and may generate other radicals, including superoxide (Reaction 2).

$$O_{2\,(aq)} + AscH_2 \rightarrow AscH^• + O_2^{•-} + H^+ \quad [2]$$

Only $AscH^•$ was observed in the EPR spectrum (not superoxide, $^•OH$, or other species; Figure 5B), but our instrument is not sensitive enough to detect low radical concentrations that may cause DNA damage. For example, 500-fold more concentrated H_2O_2 was used for EPR studies than in the gel electrophoresis studies to generate enough radicals to be easily identified. In contrast, ascorbate concentrations were similar (depending on the reaction time).

Alternatively, H_2O_2 generation from a two-electron reduction of O_2 has been proposed (Morgan *et al.* 1976), as well as reduction of Cu^{2+} by ascorbate to initiate the Fenton-like reaction (Reaction 1). H_2O_2 generation also may occur from ascorbate oxidation catalyzed by Cu^{2+} (Jameson and Blackburn 1982). Ascorbate oxidation by $O_2^{•-}$ to produce H_2O_2 and ultimately $^•OH$ (Lowry and O'Neill 1992) occurs with a high rate constant ($k = 10^{20}$) (Sawyer and Valentine 1981) and is reported in human lymphoma (U937) cells cultured with erythrocytes or fibroblasts (Sestili *et al.* 1996).

H_2O_2 and ascorbate—In the presence of H_2O_2 and ascorbate, the EC_{50} values for ^{NP}CuO and ^{w}CuO were generally lower than with ascorbate or H_2O_2 alone. The damage was also greater than could be explained from dissolved copper, although the difference was less dramatic than with ascorbate (because dissolved copper with H_2O_2 causes more damage than with ascorbate). EPR spectra show, $OH^•$, and $O_2^{•-}$; superoxide was not observed when H_2O_2 or ascorbate were added individually. However, we cannot rule out generation of low $^•OH$, $AscH^•$, or $O_2^{•-}$ concentrations that might explain the DNA damage results.

Hydroxyl radical ($^•OH$) may also be generated by $Cu^{2+} + O_2^{•-} + H_2O_2$ in the Haber-Weiss process (Reactions 2–4) (Kehrer 2000). Theoretical models describe formation of $O_2^{•-}$, which disproportionates in protic solvents to yield H_2O_2 ($K_{(pH\,7)} = 4 \times 10^{20}$) (Sawyer and Valentine 1981), with a reduction potential at pH 7 of 0.94 ± 0.02 V (Wood 1974) and formation of $^•OOH$ as an intermediate (Bielski 1978). Detection of $^•OOH$ in our EPR experiments supports this model, and $^•OOH$ can cause DNA nicks, alone (Dix *et al.* 1996) or bound to Cu^+ (Yamamoto and Kawanishi 1989; Schweigert *et al.* 2000). The reduction potential for $O_2^{•-}$ formation from O_2 is a thermodynamically unfavorable −0.33 V (Koppenol 1990; Wood 1974), but taking into account O_2 solubility (195 μM at 37 °C, 21 kPa at an ionic strength of 0.15 M), this reduction potential increases to −0.18 V (Koppenol *et al.* 2010), making $O_2^{•-}$ generation from O_2 more likely. Since ^{NP}CuO (20 – 30 nm diameter) reduction potentials range between −4.12 and −4.84 V (Atha *et al.* 2012), $O_2^{•-}$ formation is even more favorable. Adsorption of O_2 on ^{NP}CuO surfaces may also facilitate electron transfer from the conduction band to form $O_2^{•-}$ under conditions similar to our EPR experiments.

Author Manuscript Author Manuscript Author Manuscript Author Manuscript

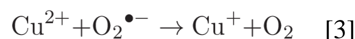

$$Cu^{2+} + O_2^{\bullet -} \rightarrow Cu^{+} + O_2 \quad [3]$$

$$O_2^{\bullet -} + H_2O_2 \rightarrow + HO^{-} + HO^{\bullet} \quad [4]$$

Both prooxidant and antioxidant activity is observed for ascorbate in ^{I}CuO + ascorbate + H_2O_2-mediated DNA damage assays. Low concentrations of ascorbate (0.0125 – 12.5 μM) reduce Cu^{2+} to Cu^{+}, resulting in $^{\bullet}OH$ formation and DNA damage (EC_{50} = 337 and 514 μM for 30 and 150 min treatment, respectively). However, ascorbate at high concentrations (1.25 – 1250 μM) acts as an antioxidant, likely by quenching its own radical, preventing DNA damage and increasing the EC_{50} value (Table 1). In the presence of ascorbate or ascorbate + H_2O_2, $AscH^{\bullet}$ is also observed (Figures 5B and 5C). $AscH^{\bullet}$ may donate one electron to dioxygen to generate $O_2^{\bullet -}$ (reaction 2) and, in the presence of copper, H_2O_2 and $^{\bullet}OH$ (reactions 3 – 4) (Cross *et al.* 2003; Li, Zhu, *et al.* 2012). High ascorbate concentrations make this reaction potential positive and thermodynamically favorable (Zhao and Jung 1995). DNA damage and $O_2^{\bullet -}$, $^{1}O_2$, and $^{\bullet}OH$ formation by treatment with ascorbate and O_2 is reported (Morgan *et al.* 1976). In addition, ROS may be generated by other mechanisms, including electron transfer from the nanoparticle conduction band to ascorbate, as proposed for redox cycling of glutathione and catalase by ^{NP}CuO (Atha *et al.* 2012).

Prooxidant behavior of ascorbate and $AscH^{\bullet}$-derived products can cause DNA damage (Kimoto *et al.* 1993) and deoxyribose degradation by $^{\bullet}OH$ (Zhao and Jung 1995). Cu^{2+} with ascorbate and O_2 more effectively kills *Bacillus globigii* spores than the Fenton-like reaction (reaction 1), and killing effectiveness is reduced in the absence of O_2 (Cross *et al.* 2003). Ascorbate oxidation is also inhibited without O_2 (Mystkowski 1942).

Other proposed DNA-damaging mechanisms include formation of a DNA/Cu^{2+}/H_2O_2 complex or Cu^{2+}-bound $^{\bullet}OH$ as the damaging species (Yamamoto and Kawanishi 1989). $^{1}O_2$ may form in the presence of ^{NP}CuO under oxidative stress conditions (Jose *et al.* 2011; Li, Zhang, *et al.* 2012), and this ROS also decomposes into $^{\bullet}OH$ (Lion and Van De Horst 1980). We detected $^{1}O_2$ generated from Cu^{2+} + ascorbate + H_2O_2 using high Cu^{2+} concentration (300 μM); thus, it is possible that $^{1}O_2$ also forms from dissolved copper of ^{NP}CuO but in amounts undetectable by EPR spectroscopy with our concentrations of dissolved copper. However, $^{1}O_2$ generation from $O_2^{\bullet -}$ is reported, and might also be occurring under our DNA damage conditions (Khan and Kasha 1994; Ueda *et al.* 2003). These reports indicate $^{\bullet}OH$ generation by different pathways, and support ROS generation by the nanoparticle core (Karlsson, Cronholm, *et al.* 2008; Atha *et al.* 2012; Cronholm *et al.* 2013; Karlsson *et al.* 2009; Karlsson, Holgersson, *et al.* 2008; Kasemets *et al.* 2009; Studer *et al.* 2010), consistent with our results.

Relative effect from the surface

^{NP}CuO toxicity assayed in human cells, *E. coli*, rainbow trout, and crustaceans has been primarily attributed to dissolved copper, but toxicity from the ^{NP}CuO surfaces has also been

Author Manuscript Author Manuscript Author Manuscript Author Manuscript

reported (Karlsson, Cronholm*, et al.* 2008; Blinova *et al.* 2010; Gunawan *et al.* 2011; Heinlaan *et al.* 2008; Isani *et al.* 2013). Many factors affect toxicity of ^{NP}CuO in cells and organisms, including uptake rate, compartmentalization in lysozomes or other organelles, changes in pH, redox status of the cell or organelle, and interactions with copper-binding or redox-active biomolecules such as glutathione. Our in-vitro measurements avoid these confounding factors while still measuring DNA damage as a biologically relevant endpoint.

Our results demonstrate that the nanoparticle surface generates DNA-damaging ROS, since DNA is damaged by ^{w}CuO + ascorbate + H_2O_2 (EC_{50} = 69 μM). ^{NP}CuO is more DNA-damaging than ^{w}CuO under the same conditions. Moreover, only a small portion of the difference between ^{w}CuO and ^{NP}CuO DNA-damaging capacities can be explained by removal of dissolved copper. Since approximately 4% of the copper ions in ^{NP}CuO are on the surface (calculation in Figure S29), the concentration of surface copper is significantly lower than nanoparticle concentrations (Table 1). In fact, 4% of the EC_{50} values for 150 min treatment with ^{NP}CuO + ascorbate + H_2O_2 (27.8 μM) or ^{w}CuO + ascorbate + H_2O_2 (69 μM) are 1.1 and 2.8 μM, respectively, similar to the EC_{50} value of dissolved copper (1.6 μM) under these conditions. This calculation treats all surface sites equally and does not address whether some crystal facets or corner sites may be more catalytically active than others. Overall, the results indicate that in the presence of ascorbate (or ascorbate and H_2O_2) the average surface site is approximately as damaging to DNA as dissolved copper, and overall damage depends upon the amount of dissolved copper and nanoparticle surface area.

Conclusions

^{NP}CuO cause DNA damage by $^{\bullet}$OH generation on the surface of CuO nanoparticles (^{w}CuO) and from dissolved copper (^{l}CuO) fractions by reaction mechanisms that involve $O_2^{\bullet-}$ and ascorbyl radical in addition to $^{\bullet}$OH generation. This DNA damage is time-dependent and increases upon addition of ascorbate and/or H_2O_2. Only a portion of the observed DNA damage can be explained by dissolved copper in the nanoparticle solution, so the surface of the ^{NP}CuO must contribute significantly to the observed damage. Knowing the capacity of different ^{NP}CuO components to cause DNA damage that leads to cellular toxicity and apoptosis may facilitate development of techniques and therapies to reduce the adverse effects of ^{NP}CuO exposure (or enhance antimicrobial properties) and allow us to take better advantage of this material in a wide variety of industrial and other applications.

Supplementary Material

Refer to Web version on PubMed Central for supplementary material.

Acknowledgments

We thank the National Institutes of Health (NIH-NIBIB 1R15EB014560) for financial support. Electron microscopy characterization was supported The South Carolina Bioengineering Center of Regeneration and Formation of Tissues (BioCRAFT) center funded under NIGMS of the National Institutes of Health, award number 5P20GM103444-07. C.A.M and K.V.T.N. thank the Clemson University Chemistry Department for graduate fellowships. C.A.M. thanks the Department of Science of the Government of Costa Rica for a graduate fellowship. K.V.T.N. received support from the Vietnam Education Foundation fellowship.

Author Manuscript
Author Manuscript
Author Manuscript
Author Manuscript

References

Alves D, Santos CG, Paixao MW, Soares LC, De Souza D, Rodrigues OED, Braga AL. CuO nanoparticles: An efficient and recyclable catalyst for cross-coupling reactions of organic diselenides with aryl boronic acids. Tetrahedron Lett. 2009; 50:6635–6638.

Angelé-Martínez CGC, Brumaghim JL. Metal-mediated DNA damage and cell death: Mechanisms, detection methods, and cellular consequences. Metallomics. 2014; 6:1358–1381. [PubMed: 24788233]

Atha DH, Wang H, Petersen EJ, Cleveland D, Holbrook RD, Jaruga P, Dizdaroglu M, Xing B, Nelson BC. Copper oxide nanoparticle mediated DNA damage in terrestrial plant models. Environ Sci Technol. 2012; 46:1819–1827. [PubMed: 22201446]

Bartosz G. Use of spectroscopic probes for detection of reactive oxygen species. Clin Chim Acta. 2006; 368:53–76. [PubMed: 16483560]

Bielski BHJ. Reevaluation of the spectral and kinetic properties of HO_2 and O_2^- free radicals. Photochem Photobiol. 1978; 28:645–649.

Blinova I, Ivask A, Heinlaan M, Mortimer M, Kahru A. Ecotoxicity of nanoparticles of CuO and ZnO in natural water. Environ Pollut. 2010; 158:41–47. [PubMed: 19800155]

Bondarenko O, Juganson K, Ivask A, Kasemets K, Mortimer M, Kahru A. Toxicity of Ag, CuO and ZnO nanoparticles to selected environmentally relevant test organisms and mammalian cells in vitro: A critical review. Arch Toxicol. 2013; 87:1181–1200. [PubMed: 23728526]

Burgess RC, Misteli T, Oberdoerffer P. DNA damage, chromatin, and transcription: The trinity of aging. Curr Opin Cell Biol. 2012; 24:724–730. [PubMed: 22902297]

Cadena E. Basic mechanisms of antioxidant activity. BioFactors. 1997; 6:391–397. [PubMed: 9388304]

Cho WS, Duffin R, Thielbeer F, Bradley M, Megson IL, Macnee W, Poland CA, Tran CL, Donaldson K. Zeta potential and solubility to toxic ions as mechanisms of lung inflammation caused by metal/metal oxide nanoparticles. Toxicol Sci. 2012; 126:469–477. [PubMed: 22240982]

Clément JL, Ferré N, Siri D, Karoui H, Rockenbauer A, Tordo P. Assignment of the EPR spectrum of 5,5-dimethyl-1-pyrroline-N-oxicdde (DMPO) superoxide spin adduct. J Org Chem. 2004; 70:1198–1203.

Cooke MS, Evans MD, Dizdaroglu M, Lunec J. Oxidative DNA damage: Mechanisms, mutation, and disease. FASEB J. 2003; 17:1195–1214. [PubMed: 12832285]

Cooney TE. Bactericidal activity of copper and noncopper paints. Infect Control Hosp Epidemiol. 1995; 16:444–450. [PubMed: 7594390]

Cronholm P, Karlsson HL, Hedberg J, Lowe TA, Winnberg L, Elihn K, Wallinder IO, Moller L. Intracellular uptake and toxicity of Ag and CuO nanoparticles: A comparison between nanoparticles and their corresponding metal ions. Small. 2013; 9:970–982. [PubMed: 23296910]

Cross JB, Currier RP, Torraco DJ, Vanderberg LA, Wagner GL, Gladen PD. Killing of *Bacillus* spores by aqueous dissolved oxygen, ascorbic acid, and copper ions. Appl Environ Microbiol. 2003; 69:2245–2252. [PubMed: 12676707]

Dix TA, Hess KM, Medina MA, Sullivan RW, Tilly SL, Webb TL. Mechanism of site-selective DNA nicking by the hydrodioxyl (perhydroxyl) radical. Biochemistry. 1996; 35:4578–4783. [PubMed: 8605208]

Eaton, AD., Ciesceri, LS., Rice, EW., Greenberg, AE. Standard Methods for the Examination of Water and Wastewater. Washington, D.C: American Public Health Association; 2001.

Fufezan C, Rutherford AW, Krieger-Liszkay A. Singlet oxygen production in herbicide-treated photosystem II. FEBS Lett. 2002; 532:407–410. [PubMed: 12482601]

Gaetke LMC-J, HS, Chow CK. Copper: toxicological relevance and mechanisms. Arch Toxicol. 2014; 88:1929–1938. [PubMed: 25199685]

Grassian VH. When size really matters: Size-dependent properties and surface chemistry of metal and metal oxide nanoparticles in gas and liquid phase environments. J Phys Chem C. 2008; 112:18303–18313.

Author Manuscript Author Manuscript Author Manuscript Author Manuscript

Gunawan C, Teoh WY, Marquis CP, Amal R. Cytotoxic origin of copper(II) oxide nanoparticles: comparative studies with micron-sized particles, leachate, and metal salts. ACS Nano. 2011; 5:7214–7225. [PubMed: 21812479]

Heinlaan M, Ivask A, Blinova I, Dubourguier HC, Kahru A. Toxicity of nanosized and bulk ZnO, CuO and TiO_2 to bacteria *Vibrio fischeri* and crustaceans *Daphnia magna* and *Thamnocephalus platyurus*. Chemosphere. 2008; 71:1308–1316. [PubMed: 18194809]

Henle ES, Han Z, Tang N, Rai P, Luo Y, Linn S. Sequence-specific DNA cleavage by Fe^{2+}-mediated fenton reactions has possible biological implications. J Biol Chem. 1999; 274:962–971. [PubMed: 9873038]

Hertzberg RP, Dervan PB. Cleavage of double helical DNA by methidium-propyl-EDTA-iron(II). J Am Chem Soc. 1982; 104:313–315.

Ide T, Tsutsui H, Hayashidani S, Kang D, Suematsu N, Nakamura K, Utsumi H, Hamasaki N, Takeshita A. Mitochondrial DNA damage and dysfunction associated with oxidative stress in failing hearts after myocardial infarction. Circ Res. 2001; 88:529–535. [PubMed: 11249877]

Isani G, Falcioni ML, Barucca G, Sekar D, Andreani G, Carpene E, Falcioni G. Comparative toxicity of CuO nanoparticles and $CuSO_4$ in rainbow trout. Ecotoxicol Environ Saf. 2013; 97:40–46. [PubMed: 23932511]

Iyanagi T, Yamazaki I, Anan KF. One-electron oxidation-reduction properties af ascorbic acid. Biochim Biophys Acta. 1985; 806:255–261.

Jameson RF, Blackburn NJ. The copper-catalysed oxidation of ascorbic acid by dioxygen. Part 4. The effect of chloride ions on the kinetics and mechanism. J Chem Soc, Dalton Trans. 1982:9–13.

Jo HJ, Choi JW, Lee SH, Hong SW. Acute toxicity of Ag and CuO nanoparticle suspensions against *Daphnia magna*: The importance of their dissolved fraction varying with preparation methods. J Hazard Mater. 2012; 227–228:301–308.

Jose GP, Santra S, Mandal SK, Sengupta TK. Singlet oxygen mediated DNA degradation by copper nanoparticles: potential towards cytotoxic effect on cancer cells. J Nanobiotechnology. 2011; 9(1–8):9. [PubMed: 21439072]

Karlsson HL, Cronholm P, Gustafsson J, Moller L. Copper oxide nanoparticles are highly toxic: A comparison between metal oxide nanoparticles and carbon nanotubes. Chem Res Toxicol. 2008; 21:1726–1732. [PubMed: 18710264]

Karlsson HL, Gustafsson J, Cronholm P, Moller L. Size-dependent toxicity of metal oxide particles--a comparison between nano- and micrometer size. Toxicol Lett. 2009; 188:112–118. [PubMed: 19446243]

Karlsson HL, Holgersson A, Moller L. Mechanisms related to the genotoxicity of particles in the subway and from other sources. Chem Res Toxicol. 2008; 21:726–731. [PubMed: 18260651]

Kartal SN, Green F III, Clausen CA. Do the unique properties of nanometals affect leachability or efficacy against fungi and termites? Int Biodeterior Biodegradation. 2009; 63:490–495.

Kasemets K, Ivask A, Dubourguier HC, Kahru A. Toxicity of nanoparticles ZnO, CuO and TiO_2 to yeast *Saccharomyces cerevisiae*. Toxicol In Vitro. 2009; 23:1116–1122. [PubMed: 19486936]

Kehrer JP. The Haber-Weiss reaction and mechanisms of toxicity. Toxicology. 2000; 149:43–50. [PubMed: 10963860]

Keyer K, Gort AS, Imlay JA. Superoxide and the production of oxidative DNA damage. J Bacteriol. 1995; 177:6782–6790. [PubMed: 7592468]

Khan AU, Kasha M. Singlet molecular oxygen in the Haber-Weiss reaction. Proc Natl Acad Sci USA. 1994; 91:12365–12367. [PubMed: 7809042]

Kimoto E, Tanaka H, Ohmoto T, Choami M. Analysis of the transformation products of dehydro-L-ascorbic acid by ion-pairing high-performance liquid chromatography. Anal Biochem. 1993; 214:38–44. [PubMed: 8250252]

Koppenol WH. Oxyradical reactions: From bond-dissociation energies to reduction potentials. FEBS Lett. 1990; 264:165–167. [PubMed: 2358063]

Koppenol WH, Stanbury DM, Bounds PL. Electrode potentials of partially reduced oxygen species, from dioxygen to water. Free Radic Biol Med. 2010; 49:317–322. [PubMed: 20406682]

Author Manuscript Author Manuscript Author Manuscript Author Manuscript

Li Y, Zhang W, Niu J, Chen Y. Mechanism of photogenerated reactive oxygen species and correlation with the antibacterial properties of engineered metal-oxide nanoparticles. ACS Nano. 2012; 6:5164–5173. [PubMed: 22587225]

Li Y, Zhu T, Zhao J, Xu B. Interactive enhancements of ascorbic acid and iron in hydroxyl radical generation in quinone redox cycling. Environ Sci Technol. 2012; 46:10302–10309. [PubMed: 22891791]

Lion Y, Van De Horst A. On the production of nitroxide radicals by singlet oxygen reaction. Photochem Photbiol. 1980; 31:305–309.

Lowry JP, O'Neill RD. Homogeneous mechanism of ascorbic acid interference in hydrogen peroxide detection at enzyme-modified electrodes. Anal Chem. 1992; 64:453–456. [PubMed: 1616131]

Luijsterburg MS, Van Attikum H. Chromatin and the DNA damage response: The cancer connection. Mol Oncol. 2011; 5:349–367. [PubMed: 21782533]

Luyts K, Napierska D, Nemery B, Hoet PHM. How physico-chemical characteristics of nanoparticles cause their toxicity: complex and unresolved interrelations. Environm Sci Processes Impacts. 2013; 15:23–38.

Mani RG, Smet JH, Von Klitzing K, Narayanamurti V, Johnson WB, Umansky V. Demonstration of a 1/4-cycle phase shift in the radiation-induced oscillatory magnetoresistance in GaAs/AlGaAs devices. Phys Rev Lett. 2004; 92:146801–146805. [PubMed: 15089564]

Maurer-Jones MA, Gunsolus IL, Murphy CJ, Haynes CL. Toxicity of engineered nanoparticles in the environment. Anal Chem. 2013; 85:3036–3049. [PubMed: 23427995]

Morgan AR, Cone RL, Elgert TM. The mechanism of DNA strand breakage by vitamin C and superoxide and the protective roles of catalase and superoxide dismutase. Nucleic Acids Res. 1976; 3:1139–1149. [PubMed: 181730]

Moshe TB, Dror I, Berkowitz B. Oxidation of organic pollutants in aqueous solutions by nanosized copper oxide catalysts. Appl Cat, B. 2009; 85:207–211.

Mouithys-Mickalad A, Deby C, Deby-Dupont G, Lamy M. An electron spin resonance (ESR) study on the mechanism of ascorbyl radical production by metal-binding proteins. BioMetals. 1998; 11:81–88. [PubMed: 9542060]

Mystkowski EM. The oxidation of ascorbic acid in the presence of copper. Biochem J. 1942; 36:494–500. [PubMed: 16747551]

Ren G, Hu D, Cheng EW, Vargas-Reus MA, Reip P, Allaker RP. Characterisation of copper oxide nanoparticles for antimicrobial applications. Int J Antimicrob Agents. 2009; 33:587–590. [PubMed: 19195845]

Rim KT, Song SW, Kim HY. Oxidative DNA Damage from Nanoparticle Exposure and Its Application to Workers' Health: A Literature Review. Saf Health Work. 2013; 4:177–186. [PubMed: 24422173]

Sawyer DT, Valentine JS. How Super is Superoxide. Acc Chem Res. 1981; 14:393–400.

Scherrer P. Bestimmung der grösse und der inneren struktur von kolloidteilchen mittels röntgenstrahlen. Göttinger Nachrichten Gessell. 1918; 2:98–100.

Schweigert N, Acero JL, Von Gunten U, Canonica S, Zehnder AJ, Eggen RI. DNA degradation by the mixture of copper and catechol is caused by DNA-copper-hydroperoxo complexes, probably DNA-Cu(I)OOH. Environ Mol Mutagen. 2000; 36:5–12. [PubMed: 10918354]

Selvakumar P, Suresh S. Conective performance of CuO/ater nanofluid in an electronic heat sink. Exp Thermal Fluid Sci. 2012; 40:57–63.

Sestili P, Brandi G, Brambilla L, Cattabeni F, Cantoni O. Hydrogen peroxide mediates the killing of U937 tumor cells elicited by pharmacologically attainable concentrations of ascorbic acid: Cell death prevention by extracellular catalase or catalase from cocultured erythrocytes or fibroblasts. J Pharmacol Exp Ther. 1996; 277:1719–1725. [PubMed: 8667243]

Shi J, Abid AD, Kennedy IM, Hristova KR, Silk WK. To duckweeds (*Landoltia punctata*), nanoparticulate copper oxide is more inhibitory than the soluble copper in the bulk solution. Environ Pollut. 2011; 159:1277–1282. [PubMed: 21333422]

Stockel J, Safar J, Wallace AC, Cohen FE, Prusiner SB. Prion protein selectively binds copper(II) ions. Biochemistry. 1998; 37:7185–7193. [PubMed: 9585530]

Studer AM, Limbach LK, Van Duc L, Krumeich F, Athanassiou EK, Gerber LC, Moch H, Stark WJ. Nanoparticle cytotoxicity depends on intracellular solubility: Comparison of stabilized copper metal and degradable copper oxide nanoparticles. Toxicol Lett. 2010; 197:169–174. [PubMed: 20621582]

Thit A, Selck H, Bjerregaard HF. Toxicity of CuO nanoparticles and Cu ions to tight epithelial cells from *Xenopus laevis* (A6): Effects on proliferation, cell cycle progression and cell death. Toxicol In Vitro. 2013; 27:1596–1601. [PubMed: 23268107]

Ueda J, Takeshita K, Matsumoto S, Yazaki K, Kawaguchi M, Ozawa T. Singlet oxygen-mediated hydroxyl radical production in the presence of phenols: whether DMPO-*OH formation really indicates production of *OH? Photochem Photobiol. 2003; 77:165–170. [PubMed: 12785055]

Vajjha RS, Das DK, Kulkarni D. Development of new correlations for convective heat transfer and friction factor in turbulent regime for nanofluids. Int J Heat Mass Transfer. 2010; 53:4607–4618.

Valko M, Morris H, Cronin MT. Metals, toxicity and oxidative stress. Curr Med Chem. 2005; 12:1161–1208. [PubMed: 15892631]

Villamena FA, Zweier JL. Detection of reactive oxygen and nitrogen species by EPR spin trapping. Antioxid Redox Signal. 2004; 6:619–629. [PubMed: 15130289]

Wang Z, Li N, Zhao J, White JC, Qu P, Xing B. CuO nanoparticle interaction with human epithelial cells: Cellular uptake, location, export, and genotoxicity. Chem Res Toxicol. 2012; 25:1512–1521. [PubMed: 22686560]

Wood PM. The redox potential of the system oxygen-superoxide. FEBS Lett. 1974; 44:22–24. [PubMed: 4855030]

Yamamoto K, Kawanishi S. Hydroxyl free radical is not the main active species in site-specific DNA damage induced by copper (II) ion and hydrogen peroxide. J Biol Chem. 1989; 264:15435–15440. [PubMed: 2549063]

Zhao MJ, Jung L. Kinetics of the competitive degradation of deoxyribose and other molecules by hydroxyl radicals produced by the Fenton reaction in the presence of ascorbic acid. Free Radic Res. 1995; 23:229–243. [PubMed: 7581818]

Author Manuscript
Author Manuscript
Author Manuscript
Author Manuscript

Author Manuscript Author Manuscript Author Manuscript Author Manuscript

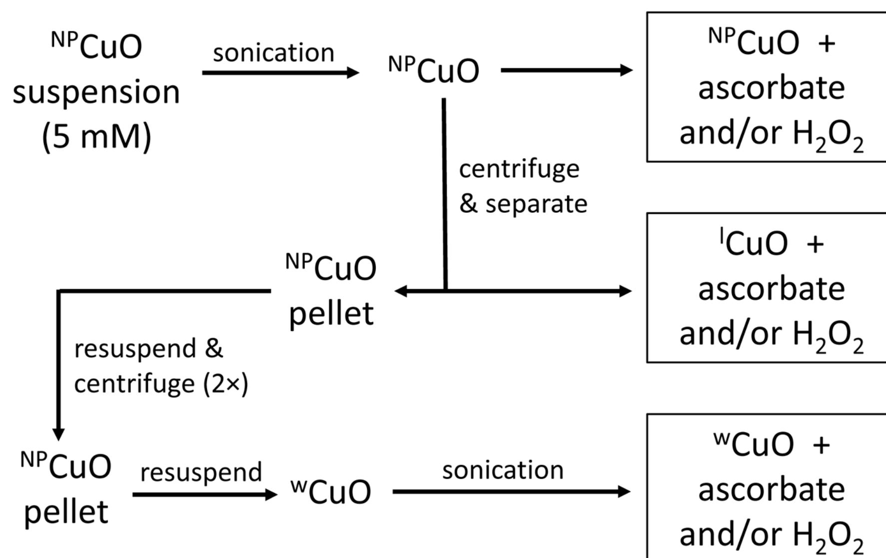

Figure 1.
Flowchart illustrating separation of ^{NP}CuO components to evaluate DNA damage. ^{NP}CuO: whole suspension of CuO nanoparticles, ^{w}CuO: washed CuO nanoparticles, ^{l}CuO: leachate of CuO nanoparticles.

Author Manuscript

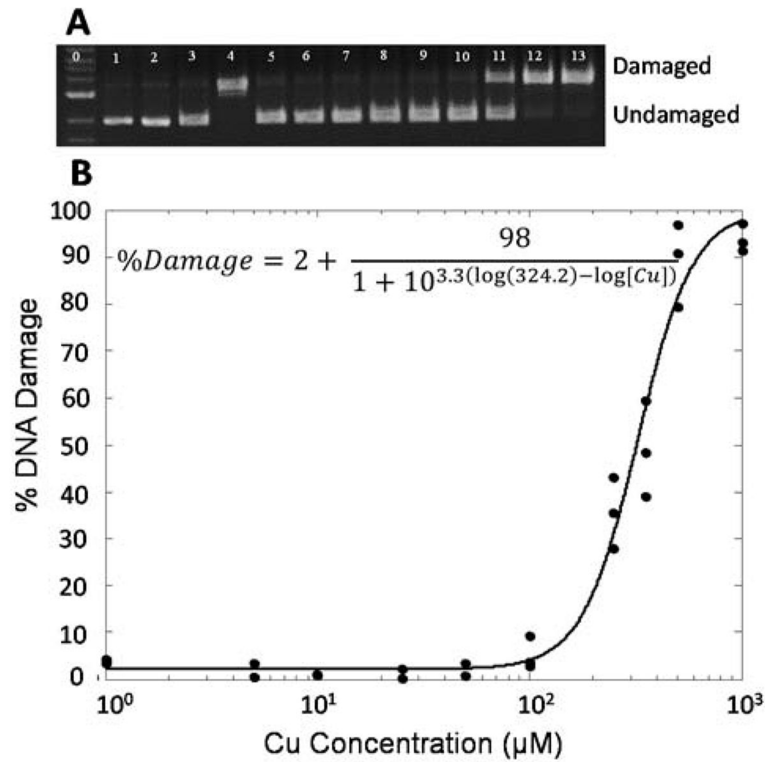

Figure 2.

A) Gel electrophoresis image of plasmid DNA (p) treated with ^{NP}CuO (1–1000 μM) and H_2O_2 (50 μM) for 150 min at pH 7 (MOPS, 10 mM). Lane 0: 1 kb molecular weight ladder; 1: p; 2: p + H_2O_2 (50 μM), 3: p + ^{NP}CuO (1000 μM); 4: p + Cu^{2+} (6 μM) + ascorbate (7.5 μM) + H_2O_2 (50 μM); lanes 5–13: p + H_2O_2 (50 μM) + increasing concentrations of ^{NP}CuO (1, 5, 10, 25, 50, 100, 250, 500, and 1000 μM, respectively). B) Dose-response curve fitting for the gel data in A to obtain an EC_{50} value.

Author Manuscript
Author Manuscript
Author Manuscript
Author Manuscript

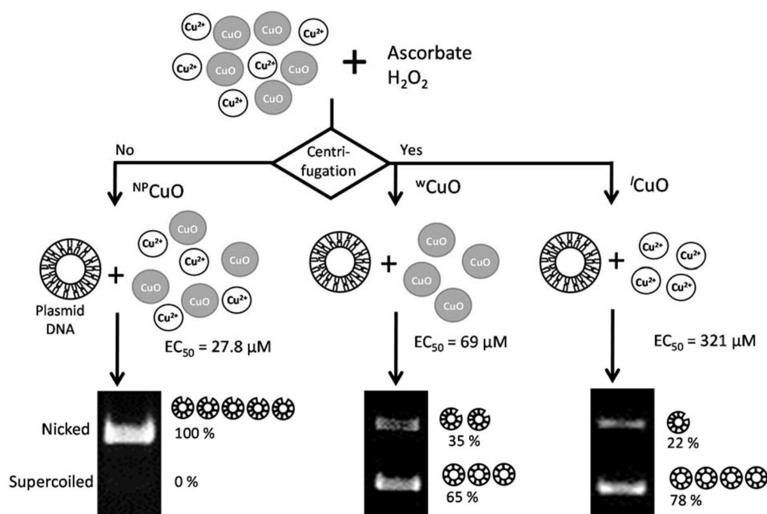

Figure 3.

Comparative scheme of DNA damage (shown in gel images) caused by ^{NP}CuO, ^{w}CuO, and ^{l}CuO fractions (50 µM) with ascorbate and H_2O_2 for 150 min.

Author Manuscript
Author Manuscript
Author Manuscript
Author Manuscript

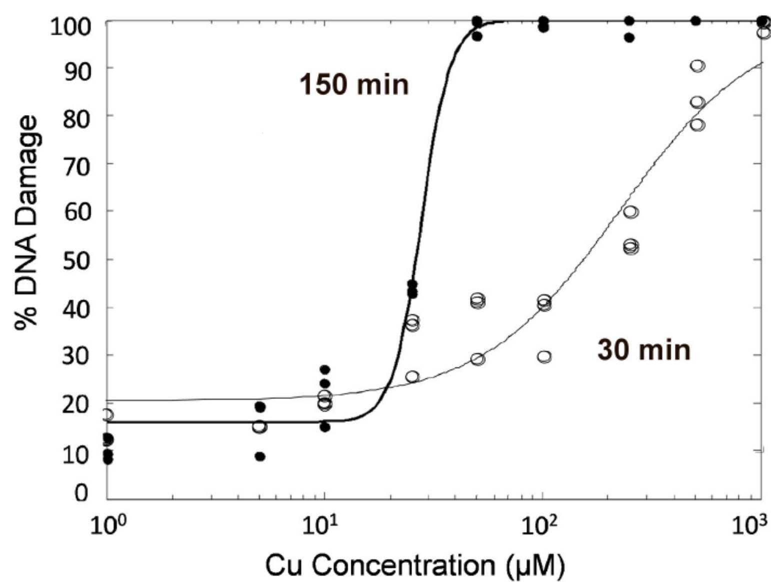

Figure 4.

Comparison of the EC_{50} plots for DNA damage caused by ^{NP}CuO, ascorbate (1.25 equiv; 1.25 – 1250 μM), and H_2O_2 (50 μM) for 30 min (open circles) and 150 min (filled circles).

Author Manuscript Author Manuscript Author Manuscript Author Manuscript

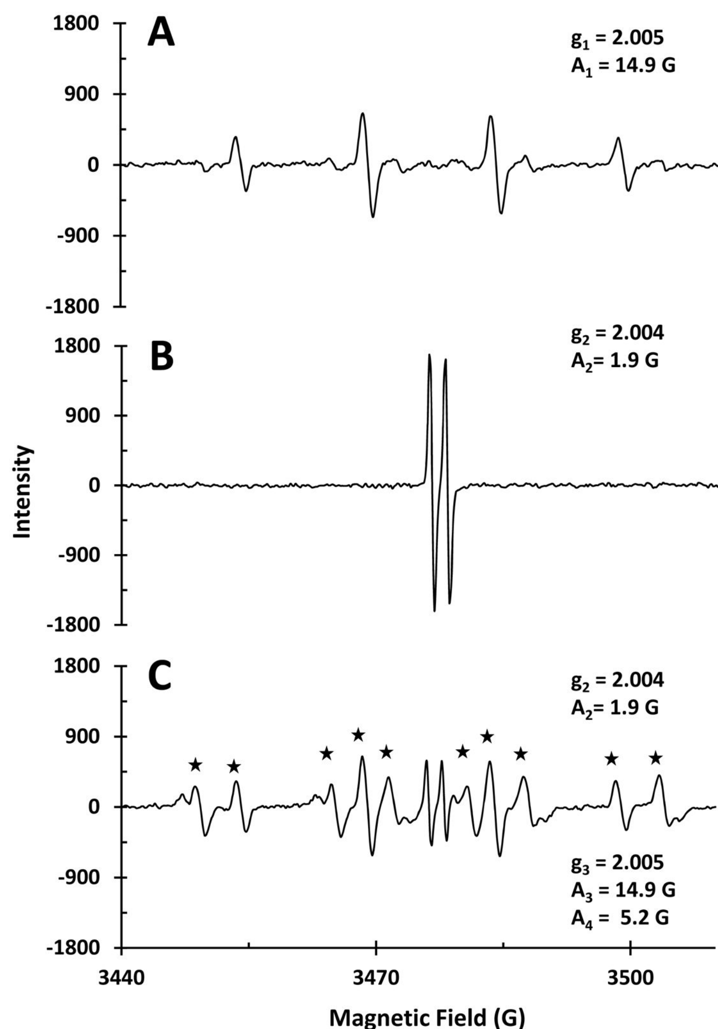

Figure 5.

EPR spectra of ^{w}CuO (300 μM) with A) H_2O_2 (22.5 mM), B) ascorbate (375 μM), and C) H_2O_2 (22.5 mM) and ascorbate (375 μM). All samples in buffer at pH 7 (MOPS, 10 mM) with DMPO (30 mM) as a spin trap. Asterisks indicate DMPO-OOH resonances. A_1 and g_1; A_2 and g_2; and g_3 and A_3 correspond to DMPO-OH, AscH$^{\bullet}$, and DMPO-OOH resonances, respectively. A_4 is the second hyperfine coupling constant for the DMPO-OOH resonance.

Author Manuscript
Author Manuscript
Author Manuscript
Author Manuscript

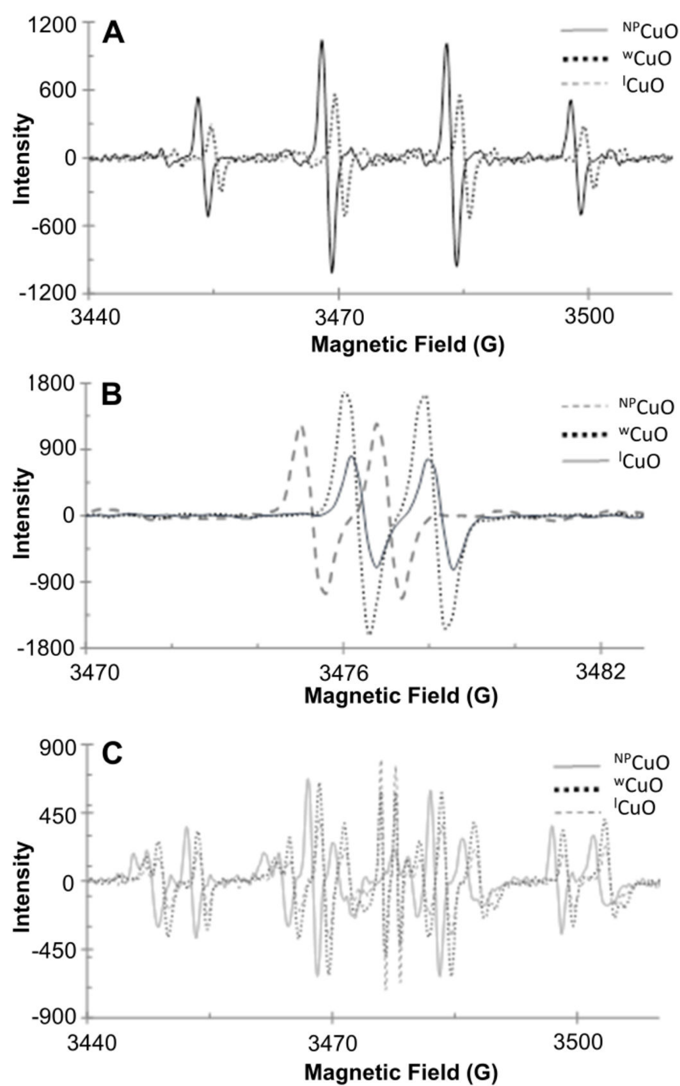

Figure 6.

Comparison of EPR spectra with CuO fractions (^{NP}CuO, ^{w}CuO, or ^{l}CuO; 300 μM) and A) H_2O_2 (22.5 mM), B) ascorbate (375 μM), or C) H_2O_2 (22.5 mM) and ascorbate (375 μM). All samples in buffer at pH 7 (MOPS, 10 mM) with DMPO (30 mM) as a spin trap.

Author Manuscript

Author Manuscript

Author Manuscript

Author Manuscript

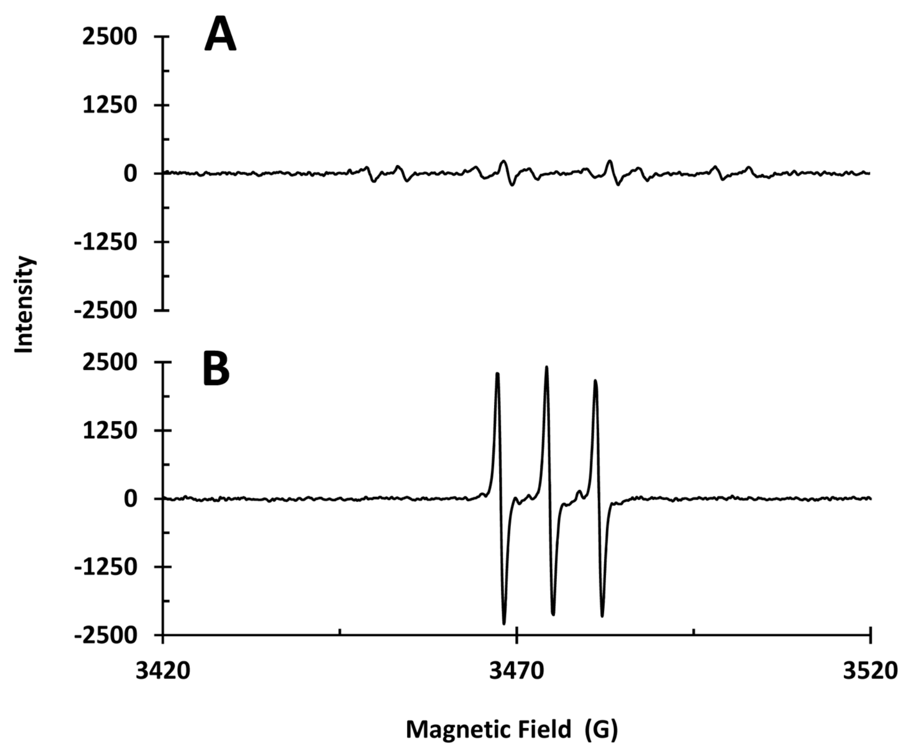

Figure 7.

EPR spectra of $CuSO_4$ (300 μM),H_2O_2 (22.5 mM), and ascorbate using A) DMPO (30 mM) and B) TEMP (30 mM) as a spin trap.

Author Manuscript Author Manuscript Author Manuscript Author Manuscript

Table 1

Concentrations required to cause 50% DNA damage (EC_{50}, μM) for solutions of CuO nanoparticles (^{NP}CuO), washed nanoparticles (^{w}CuO), leachate of ^{NP}CuO (^{l}CuO), and dissolved (free) copper (values in parentheses; μM)

Component	150 Minutes				30 Minutes		
	H_2O_2	Ascorbate (1.25 equiv)	H_2O_2 + Ascorbate (1.25 equiv)	Other Conditions	H_2O_2	Ascorbate (1.25 equiv)	H_2O_2 + Ascorbate (1.25 equiv)
^{NP}CuO	324 ± 29 (1.54)	39 ± 3 (0.13–0.39)[b]	27.8 ± 0.5 (0.09–0.28)[b]	52 ± 3[a] (0.17–0.53)[b]	> 1000	ND	223 ± 60
^{w}CuO	ND	170 ± 27 (0.22–0.82)[b]	69 ± 20 (0.09–0.34)[b]	-	ND	253 ± 8 (0.33–0.45)[b]	318 ± 37 (0.41–0.57)[b]
^{l}CuO	ND	ND	321 ± 30 (1.53)	690 ± 130[c] (3.3)	ND	> 1000	434 ± 83 (2.1)[d]
Cu^{2+}	1.5 ± 0.1	5.3 ± 0.2	1.6 ± 0.2	2.3 ± 0.2[d]	4.4 ± 0.1	10.3 ± 0.9	2.3 ± 0.2

[a]Constant ascorbate concentration (50 μM), no H_2O_2.

[b]A range is observed because copper concentrations change during these experiments.

[c]Ascorbate concentration was ~250× the concentration of dissolved copper in ^{l}CuO.

[d]Cu^{2+}, ascorbate, and H_2O_2 were added to DNA samples with ^{l}CuO from which the dissolved copper was removed; ^{l}CuO concentration corresponded to the same dilution factor for 1000 μM ^{NP}CuO.

ND = not determined.